Radiography 26 (2020) 234–239

Contents lists available at ScienceDirect

Radiography

journal homepage: www.elsevier.com/locate/radi

Comparison of double inversion recovery magnetic resonance imaging (DIR-MRI) and dynamic contrast enhanced magnetic resonance imaging (DCE-MRI) in detection of prostate cancer: A pilot study

E.N. Onwuharine*, A.J. Clark

Radiology Department, University Hospitals of North Midlands (UHNM) NHS Trust, UK

ARTICLE INFO

Article history:
Received 4 September 2019
Received in revised form
12 December 2019
Accepted 16 December 2019
Available online 6 January 2020

Keywords:
Prostate cancer (PCa)
Magnetic resonance imaging (MRI)
Double inversion recovery (DIR)
Dynamic contrast enhanced (DCE)
Lesion to normal ratio (LNR)
Multiparametric MRI (mpMRI)
Gadolinium contrast agent

ABSTRACT

Introduction: DCE-MRI is established for detecting prostate cancer (PCa). However, it requires a gadolinium contrast agent, with potential risks for patients. The application of DIR-MRI is simple and may allow cancer detection without the use of an intravenous contrast agent by differentially nullifying signal from normal and abnormal prostate tissue, creating contrast between the cancer and background normal prostate. In this pilot study we gathered data from DIR-MRI and DCE-MRI of the prostate for an equivalence trial. We also looked at how the DIR-MRI appearance varies with the aggressiveness of PCa.
Method: DIR-MRI and DCE-MRI were acquired. The images were assessed by an experienced Consultant Radiologist and a novice reporter (Radiographer). The potential PCa lesions were quantified using a lesion to normal ratio (LNR). Radiological pathological correlation was made to identify the MRI lesions that represented significant PCa. A Wilcoxon sign rank was used to compare DCE-LNR and DIR-LNR for PCa containing lesions. Pearson's correlation was used to look at the relationship between DIR-LNR and PCa grade group (aggressiveness).
Results: DCE-LNR and DIR-LNR were found to be significantly different ($Z = -5.910$, $p < 0.001$). However, a significant correlation was found between PCa grade group and DIR-LNR.
Conclusion: DIR and DCE sequences are not equivalent and significant cancer is more conspicuous on the DCE sequence. However, DIR-LNR does correlate with PCa aggressiveness.
Implications for practice: With the correlation of PCa grade group with DIR-LNR this may be a useful sequence in evaluation of the prostate; stratifying the risk of there being clinically significant PCa before biopsy is performed. Furthermore, given that DIR-LNR appears to predict PCa aggressiveness DIR might be used as part of a multiparametric MRI protocol designed to avoid biopsy.

Introduction

A significant challenge in PCa management is how to accurately distinguish aggressive cancer, requiring treatment, from indolent PCa that does not require treatment.[1–7] The Gleason scoring system is currently the gold standard measure of PCa aggressiveness.[8,9] However, it is possible during biopsy to miss foci of aggressive cancer.[8–15] It is documented that in about 30% of men who undergo radical prostatectomy for low-grade disease, PCa is upgraded from low grade to high grade disease on final pathology.[13] Hence there is a need for an alternative or adjunct method of detecting and assessing the disease.[13,16]

MRI plays a significant role in the diagnosis and staging of PCa. It has been found to be a valuable tool in differentiating chronic prostatitis in the peripheral zone or stromal hyperplastic nodules of the transition zone from PCa.[17] Many centres perform multiparametric MRI (mpMRI), including anatomic sequences such as T1 weighted imaging (T1WI) and T2 weighted imaging (T2WI), and functional sequences such as diffusion weighted imaging (DWI), Magnetic Resonance Spectroscopic Imaging (MRSI), and DCE-MRI. This is in line with European Society of Urogenital Radiology (ESUR) guidelines of 2012 as was presented by Barentsz et al.,[10] which recommend the combination of high-resolution T2WI and at least two functional MRI techniques for assessment of the

* Corresponding author.
E-mail addresses: eric.onwuharine@uhnm.nhs.uk (E.N. Onwuharine), Alexander.clark@uhnm.nhs.uk (A.J. Clark).

https://doi.org/10.1016/j.radi.2019.12.012

prostate. DWI is the preferred functional sequence. Despite the use of a contrast agent most MRI centres adopt DCE-MRI rather than MRSI as the second functional sequence. This may be due to the different technical challenges in data acquisition and data analysis.

DCE-MRI of the prostate provides useful information reliant on the vascular characteristics of normal and pathological prostate tissues. To provide contrast between normal prostate and cancer DCE-MRI relies on neo-angiogenesis accompanied by increased permeability of the endothelial barrier in cancers.[15,18] These changes in microvascularity result in earlier, increased enhancement then washout of the intravenous gadolinium containing contrast agent in PCa.[18] However, this functional MRI technique has pitfalls.[15] Normal prostate can be as well vascularised as abnormal prostate, so a comparison of pre and post gadolinium images is often insufficient to detect PCa.[10] Furthermore, a dominant limitation of DCE-MRI is lack of specificity.[15,19] Benign prostate pathology such as prostatitis and vascular benign prostatic hypertrophy (BPH) nodules can have the same enhancement characteristics as PCa reducing the specificity of DCE-MRI.[19] We have no doubt that DCE-MRI plays an important role in PCa diagnosis and management. However, some MRI centres for various reasons, do not apply the technique. Some of the problems, in addition to those mentioned above include cost, time, expertise, and variable specificity. To perform a high-quality DCE-MRI examination a good understanding of the technical aspects and limitations of image acquisition and post processing techniques are required.[15] Some patients decline contrast injection for their scan, others have known MRI contrast allergy or renal insufficiency. The exclusion of this sequence from mpMRI is currently supported by four arguments including that they do not provide a significant diagnostic gain, they add to cost which cannot be justified, there are unjustifiable risks associated with the injection of the contrast agent and they increase the duration of the examination.[18] It is desirable to find a quick and cost effective alternative sequence to DCE-MRI to complement other sequences in mpMRI prostate.

DIR-MRI is an inversion time (TI) based technique used to simultaneously nullify the signals from two different tissues when two 180° inversion pulses are applied before a conventional spin-echo acquisition.[20] Several studies have demonstrated the useful application of DIR-MRI in brain imaging, especially for multiple sclerosis (MS). In the brain, DIR-MRI sequence attenuates the cerebrospinal fluid (CSF) and the white matter, attaining a superior definition between grey and white matter.[21] Jeoung et al.,[20] demonstrated the usefulness of DIR-MRI in breast imaging. The application in breast was based on the ability of DIR-MRI to nullify signal from fat and fibroglandular tissue demonstrating breast cancer without the need for an intravenous contrast agent. As the DIR-MRI sequence is based on TI relaxation time a tumour may be distinguished from the background normal tissue by virtue of TI relaxation time differences.[20] The prostate is made up of both fibromuscular and glandular tissues which are altered in cancerous conditions resulting in different relaxation times between the cancer and normal prostate tissues.

To the best of our knowledge, there is no study that has applied DIR-MRI to evaluate the prostate gland. The application of DIR-MRI in the prostate is non-invasive and does not require a contrast agent. It is therefore simple and may allow cancer detection by nullifying signal either from normal tissue around the cancer or the cancer itself creating contrast between the cancer and background normal prostate.

In the study, we performed DIR-MRI for detection and determination of aggressiveness of PCa. The application of DIR-MRI in the prostate allowed cancer detection apparently by nullifying signal from the cancer preferentially thus creating contrast between the cancer and background normal prostate without the use of an intravenous contrast agent. The DIR sequence was optimised to demonstrate prostate anatomy and PCa. Our purpose in this pilot study was to confirm DIR-MRI can be used to evaluate the prostate gland and gather data from DIR-MRI and DCE-MRI in people with suspected PCa for an equivalence trial of PCa conspicuity on these sequences. In addition, we set out to explore if there is a correlation between DIR-MRI appearance and aggressiveness of PCa.

Method

This pilot study included a total of 150 patients with age range 53–89 years. They underwent DIR-MRI and mpMRI which included DCE-MRI. The study was IRAS registered and HRA approved. Written informed consent was obtained from all patients.

The inclusion criteria were all patients referred for prostate MRI for possible PCa, who were safe to undergo an MRI scan and able to give informed consent. Those excluded were those who were not safe for MRI, could not give informed consent or there is no suspicion of PCa.

Indications for MRI included abnormal digital rectal examination (DRE), raised Prostate-Specific Antigen (PSA) or active surveillance.

The DIR sequence is commercially available. The DIR sequence from our vendor was optimised to demonstrate prostate anatomy and PCa, particularly to create contrast between the cancer and background normal prostate. To do this it was necessary to minimize the T1 weighting and acquire images with greater T2 weighting by adjusting the range of TIs, this is known as T1-nulled DIR.[22]

Since the prostate is a water rich organ surrounded by fat, we decided as a starting point to null water and fat signal, by applying already established TIs for water and fat of 3000 ms and 450 ms respectively with a TR of 7500 ms. However, a wide range of values has been described for similar tissues.[23] We then optimised this DIR sequence, on the first 15 trial participants, by performing the sequence with varying TIs and TR to empirically determine the optimum parameters for prostate assessment. Firstly, TI1 and TR were varied in steps of 100 ms while TI2 was kept constant. Secondly, TI2 and TR were varied in steps of 20 ms and 100 ms respectively, while TI1 was kept constant. As each novel DIR sequence was acquired the clarity of prostate anatomy, PCa and the contrast between these was evaluated using the standard mpMRI prostate sequences as a visual guide. Images were assessed by an experienced consultant radiologist in prostate MRI and the optimum DIR sequence for the prostate was selected. TI values of 3400 ms (TI1) and 450 ms (TI2) and a TR value of 8000 ms were deemed optimum for prostate assessment in the context of our study question. Once the TIs and TR were established, the remaining participants were scanned using the same parameters. The acquisition parameters are shown in Table 1.

Fig. 1shows a schematic drawing of a DIR sequence. TI1 was the time interval between the two inversion pulses while TI2 was the time interval between the second 180^0 inversion pulse and the excitation 90^0 radiofrequency (RF) pulse.

MRI acquisition

All DIR-MRI and mpMRI examinations were performed using a combination of spine and eighteen channel body coils in a 3.0 T scanner (Magnetom Skyra, Siemens AG). Patients were encouraged to empty bowels before image acquisition to reduce artefacts from rectal movement and susceptibility artefact on DWI.

Table 1
Acquisition parameters.

Sequences	Slice Thickness (mm)	Dist. (%)	FOV (mm)	Phase FOV (%)	TR (Ms)	TE (Ms)	TI 1 (Ms)	TI 2 (Ms)	Phase over Sampling (%)	Slice over Sampling (%)	Matrix	Bandwidth (Hz/Px)	Phase Enc Dir	Averages
DCE	3.5	20	260	100	5.08	1.77	–	–	30	27.3	192 × 154	260	A > P	1
DIR	3	0	200	100	8000	323	3400	450	100	100	192	868	A > P	1

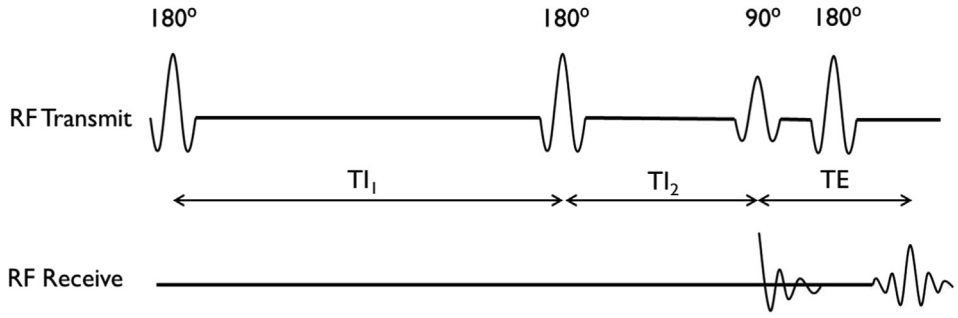

Figure 1. A schematic drawing of a DIR sequence.

Patients were asked to lay supine on the spine coil, the surface body coil was then placed on top of the pelvis. Two-dimensional (2D) T2WI in three orthogonal planes (axial, coronal, and sagittal) using T2-weighted turbo spin echo sequence, were acquired. DWI, DCE and DIR images were obtained in axial orientations. DWI was acquired using a spin echo planar imaging sequence with four b-values (0, 200, 400, and 800s/mm2). DCE images were acquired using a fast three-dimensional (3D) T1-weighted gradient echo sequence. There was an acquisition time of between 7 and 10 s on each volumetric acquisition of the DCE sequence. A total of 35 contrast-enhanced acquisitions were obtained. These followed a bolus injection of .2 mmol/kg gadoteric acid contrast agent (Dotarem, Guerbet) followed by a 20 mL flush of saline both at the rate of 3 mL/s, using a motorized power Injector (Solaris system).

DIR was acquired using a spin echo (SE) sequence with two nonselective 180° inverting pulses. For the optimum DIR image elements of the coils not over the prostate gland were turned off during DIR image acquisition. This reduces unwanted signal from the surrounding areas and fold over or phase wrap. Phase-wrap artefact, from the rectum that obscured the prostate, was common in DIR image acquisition of the prostate using these coil combinations and field of view (FOV).

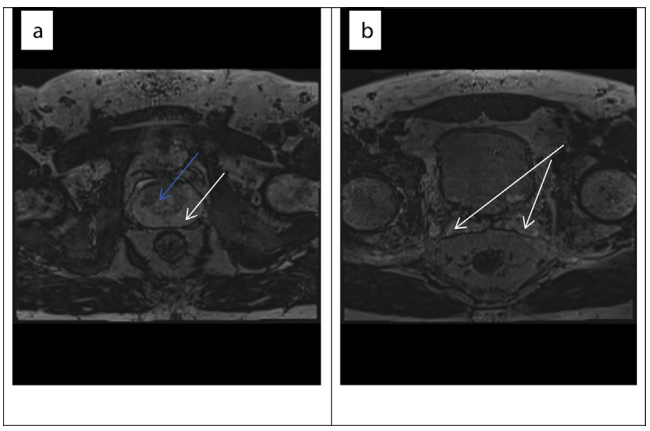

Figure 2. a) DIR demonstrating the zonal anatomy of the normal prostate; Transition zone (TZ) [blue arrow], Peripheral zone (PZ) [white arrow]. b) DIR demonstrating seminal vesicles [white arrows]. (For interpretation of the references to color in this figure legend, the reader is referred to the Web version of this article.)

Prostate biopsy

All biopsies followed MRI within a biologically insignificant time frame, a small number of weeks. Where lesions were reported on mpMRI pre-biopsy that would not be sampled by a standard set of biopsies, they were targeted at biopsy using cognitive fusion. Samples from targeted areas were labelled as such, stored separately and sent for analysis. Standard sets of transrectal biopsies were 12 cores taken from separate locations within the prostate. Biopsies from each anatomical quarter of the prostate (right apex, right base, left apex and left base) were labelled as such and stored separately. These locations were used to determine if mpMRI described lesions corresponded to significant PCa.

Image interpretation

All DICOM MR Images were downloaded from our PACS system (SYNGO), and independently interpreted by an experienced radiologist (with 5 years of pre-biopsy mpMRI prostate reporting experience) and by a novice reporter (senior MRI radiographer with over 10 years of prostate MR imaging experience but no reporting experience). A ROI within a suspected significant cancer was drawn on T2, ADC, DCE and DIR using a freehand technique. The established three sequences were used as a guide for the ROI on the DIR, although the appearance on DIR was also considered. A ROI was also drawn in ipsilateral normal looking prostate from the same zone on each of the sequences. On DCE-MRI, since there are repeated acquisitions, the time point chosen on which to measure the ROI was the acquisition on which the suspected PCa was most conspicuous, an empirical judgment. The ROI was drawn free hand at the same slice level on all sequences aiming to measure from the same area on each sequence. The average signal returned from within the suspected cancer and from the normal tissue was recorded in a spread sheet.

A LNR was calculated to determine the effectiveness of each sequence in lesion demonstration. The LNR = (SL-SN) ×100%/SN.[20] SL and SN are the mean signal of the lesion and normal ROI

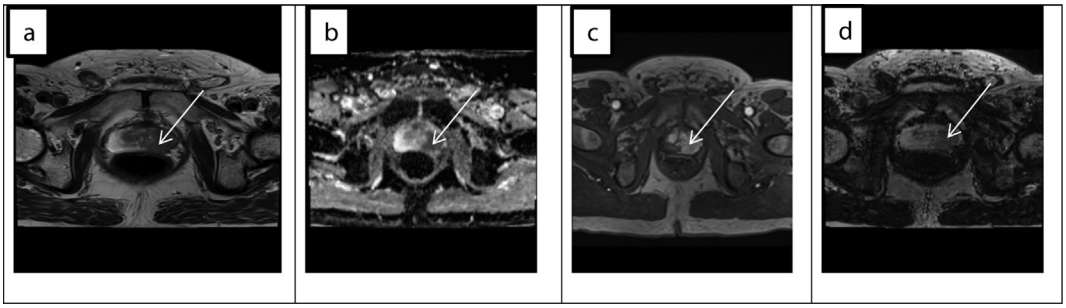

Figure 3. (a–d) Large left PZ PCa (white arrows). a) Axial T2WI. b) DWI. c) DCE. d) DIR.

respectively. When calculating the LNR for DIR-MRI the equation becomes LNR= (SN-SL) ×100%/SN. This is because on this sequence the lesion has lower signal intensity than the normal prostate.

The assessors of the scans were an experienced senior radiologist and a novice reader. The novice reader as part of the conditions for the funding received several hours of coaching to assess the scans using the PI-RADSv2 system. This system represents an established method for interpreting and reporting mpMRI prostate, providing risk stratification for clinically significant PCa.[24–27] Scores 3, 4 and 5 were taken to represent clinically significant PCa.[24,27,28] The agreement for MRI suspected significant PCa between the experienced and novice assessors was evaluated.

Histopathology results were assessed on our iportal system. Lesions identified on MRI were anatomically correlated with histopathology from biopsy (standard and targeted). Where the MRI description and biopsy location did not match or there was doubt, the lesions were not included in the analysis. The presence of cancer, Gleason grade and the grade group were recorded.

Gleason scores from 3 + 4 = 7 and higher were considered positive for significant PCa and included in the data for analysis.

Appearances of the male pelvis on DIR (as performed in the study)

An experienced radiologist, with over 10 years of experience of male pelvic MRI, assessed the appearances of the male pelvis on DIR. There was good overall demonstration of male pelvic anatomy, including zonal anatomy of the prostate, with acceptable spatial resolution.

In the pelvis, fat (including fatty bone marrow) is bright, water is intermediate to bright and muscle is intermediate to dark. The peripheral zone of the prostate is bright, the transition zone a heterogenous mosaic of predominantly well circumscribed areas of bright and intermediate signal. The seminal vesicles return a bright signal (See Fig. 2). PCa appearance is independent of the zone from which it arises and is intermediate to dark (see Fig. 3).

Data analysis

A total of 52 significant mpMRI lesions were identified that corresponded with significant cancer on biopsy and these were included in the data analysis. Data was assessed using the Shapiro–Wilk test ($p < 0.05$) (appendices A). The assumption of normality was violated for the post contrast signal in cancer and DCE-LNR. Therefore, the non-parametric alternative to a paired samples t test, a Wilcoxon Sign Rank, was performed to determine whether there was a statistically significant difference between DCE-LNR and DIR-LNR.

Pearson's correlation was used to look at the relationship of PCa grade group (derived from the Gleason grade but more clinically relevant) with mean cancer signal and LNR on the DIR sequence.

Results

The mean age of the patients was 69.57 (SD = 8.035). Table 2 shows the mean DIR signal and mean DCE signal (measured at the time of maximum LNR) returned by cancer and normal prostate including a break down of signal returned by the PZ and TZ. Table 2 also includes the mean DIR-LNR and the mean DCE-LNR.

The tumour is visible in DIR and DCE, however, it is less visible in DIR. The Wilcoxon signed rank test showed that the DCE-LNR was significantly different from the DIR-LNR ($Z = -5.910$, $p < 0.001$). This means that the two techniques are not equivalent regarding the conspicuity of cancer, DCE has the better LNR.

The consultant radiologist reported 72 significant looking MRI lesions; within which 61 significant cancers were present in 52 patients. There were 55 true positives, 45 true negatives, 17 false positives and 6 false negatives. The consultant radiologist had a sensitivity of 90.1%, specificity of 72.5% and accuracy of 81.3%.

The novice reporter reported 75 MRI significant looking lesions; within which 60 significant cancers were present in 52 patients. There were 55 true positives, 46 true negatives, 22 false positives and 6 false negatives. The novice reader has a sensitivity of 89.9%, specificity of 69.7% and accuracy = 77.9%.

Of the 150 patients, when considering a non-significant prostate MRI appearance versus an appearance suggesting significant PCa, the radiologist and novice reader agreed in 130 (86.7%) of cases.

Discussion

The main objective of this study was to determine whether DIR-MRI and DCE-MRI are equivalent in demonstrating significant PCa. Both techniques were able to demonstrate significant PCa.

Table 2
Mean Signal returned by cancer and normal prostate and LNR.

Sequence	Mean signal				
	Cancer Signal (SD)	Normal Signal (SD)			LNR (SD)
		Whole prostate	PZ	TZ	
DIR	15.27 (3.93)	23.77 (5.22)	24.71 (6.32)	19.57 (4.77)	34.22 (16.22)
DCE	303.97 (88.87)	156.85 (57.50)	154.67 (49.85)	183.21 (52.37)	104.88 (70.25)

46 men were found to have significant PCa, 6 of whom had two separate foci of PCa. The mean age for men with clinically significant PCa was 69.57 years (SD = 8.035). Several men had more than one focus of PCa and overall the number of lesions from which we calculated an LNR was 52.42 of these lesions were identified by both scan readers and the signal intensity used for the LNR was an average of that recorded by both readers.

The DIR technique has the advantage over DCE-MRI of not requiring a contrast agent, however, they are not equivalent at demonstrating PCa. Although the Wilcoxon signed rank test showed that the DCE-LNR was significantly different from the DIR-LNR, it does not mean they are not equivalent in predicting the presence of significant cancer, just that the appearance is more subtle on DIR.

A correlation between DIR-LNR and the Gleason derived grade group could be an indication that DIR is useful in determining PCa aggressiveness, and so may compliment DWI-MRI in the distinction between indolent and aggressive PCa. There is already an existing body of evidence that DWI may be useful in determining PCa aggressiveness.[29–45] A combination of DIR and DWI in mpMRI may be a significant MRI tool in determining PCa aggressiveness.

16.7% of the cancers identified appeared to originate in the TZ in this study. Not analysing PZ and TZ cancers separately is a limitation of this study that may have reduced the significance of our findings. The TZ on average has a lower signal intensity on DIR-MRI than the PZ hence there is a reduced LNR for lesions identified in this zone.

Conclusion

The results showed that DIR is not equivalent to DCE for conspicuity of PCa, it is inferior. However, there is a significant correlation between DIR-LNR and PCa grade group. This suggests that the DIR sequence may be useful in the evaluation of the prostate by predicting the presence of clinically significant PCa before biopsy is performed. Furthermore, as a sequence able to distinguish indolent from aggressive PCa DIR-MRI might be useful to decide if biopsy is needed and as a prognostic indicator when there is clinically significant PCa.

Conflict of interest statement

None.

Acknowledgments

The research was funded by The College of Radiographers Industry Partnership Scheme (CoRIPS). We would like to thank them and University Hospitals of North Midlands (UHNM) Imaging Department for funding support received in part from both.

We would also like to thank Helen Wright for her contribution in the statistical analysis of data during the study and Phil Andrews (former MRI superintendent) for ensuring a smooth patient recruitment process.

Appendix A

Tests of Normality

	Kolmogorov-Smirnov[a]			Shapiro–Wilk		
	Statistic	df	Sig.	Statistic	df	Sig.
A._Age	.079	46	.200*	.985	46	.827
B._Mean_Signal_Post_Gad_Cancer	.108	52	.192	.947	52	.022
C._Mean_Signal_Post_Gad_Normal	.116	52	.076	.962	52	.092
D._Mean_LNR_Post_Gad	.122	52	.050	.900	52	.000
E._DIR_Cancer	.104	52	.200*	.968	52	.181
F._DIR_Normal	.062	52	.200*	.990	52	.931
G._DIR_LNR	.062	52	.200*	.961	52	.085

*. This is a lower bound of the true significance.
a. Lilliefors Significance Correction.

APPENDIX B

		A. Age	B._Mean_Signal_Post_Gad_Cancer	C._Mean_Signal_Post_Gad_Normal	D._Mean_LNR_Post_Gad	E._DIR_Cancer	F._DIR_Normal	G._DIR_LNR	H._Grade_Group
A._Age	Pearson Correlation	1	-.019	-.148	.066	.047	.102	.094	.133
	Sig. (2-tailed)		.900	.325	.662	.755	.502	.533	.377
	N	46	46	46	46	46	46	46	46
B._Mean_Signal_Post_Gad_Cancer	Pearson Correlation	-.019	1	.409**	.503**	.041	.033	-.048	-.120
	Sig. (2-tailed)	.900		.003	.000	.775	.815	.733	.399
	N	46	52	52	52	52	52	52	52
C._Mean_Signal_Post_Gad_Normal	Pearson Correlation	-.148	.409**	1	-.531**	.042	-.388**	-.423**	-.325*
	Sig. (2-tailed)	.325	.003		.000	.766	.004	.002	.019
	N	46	52	52	52	52	52	52	52
D._Mean_LNR_Post_Gad	Pearson Correlation	.066	.503**	-.531**	1	-.076	.374**	.390**	.237
	Sig. (2-tailed)	.662	.000	.000		.594	.006	.004	.090
	N	46	52	52	52	52	52	52	52
E._DIR_Cancer	Pearson Correlation	.047	.041	.042	-.076	1	.510**	-.507**	-.195
	Sig. (2-tailed)	.755	.775	.766	.594		.000	.000	.166
	N	46	52	52	52	52	52	52	52
F._DIR_Normal	Pearson Correlation	.102	.033	-.388**	.374**	.510**	1	.441**	.109
	Sig. (2-tailed)	.502	.815	.004	.006	.000		.001	.444
	N	46	52	52	52	52	52	52	52

(*continued*)

		A. Age	B._Mean_Signal_ Post_Gad_Cancer	C._Mean_Signal_ Post_Gad_Normal	D._Mean_LNR_ Post_Gad	E._DIR_ Cancer	F._DIR_ Normal	G._DIR_LNR	H._Grade_ Group
G._DIR_LNR	Pearson Correlation	.094	-.048	-.423**	.390**	-.507**	.441**	1	.272
	Sig. (2-tailed)	.533	.733	.002	.004	.000	.001		.051
	N	46	52	52	52	52	52	52	52
H_Grade_Group	Pearson Correlation	.133	-.120	-.325*	.237	-.195	.109	.272	1
	Sig. (2-tailed)	.377	.399	.019	.090	.166	.444	.051	
	N	46	52	52	52	52	52	52	52

References

1. Borren A, Groenendaal G, Moman MR, Boeken KAE, Van DPJ, Van VM, et al. Accurate prostate tumour detection with multiparametric magnetic resonance imaging: dependence on histological properties. *Acta Oncol* 2014;**53**(1):88–95.
2. Diaz AW, Hoang AN, Turkbey B, Hong CW, Truong H, Sterling T, et al. Can magnetic resonance ultrasound fusion biopsy improve cancer detection in enlarged prostates? *J Urol* 2013;**190**(6):2020–5.
3. Kitajima K, Takahashi S, Ueno Y, Miyake H, Fujisawa M, Kawakami F, et al. Do apparent diffusion coefficient (ADC) values obtained using high b-values with a 3-T MRI correlate better than a transrectal ultrasound (TRUS)-guided biopsy with true Gleason scores obtained from radical prostatectomy specimens for patients with prostate cancer? *Eur J Radiol* 2013;**82**(8):1219–26.
4. Shigemura K, Yamanaka N, Yamashita M. Can diffusion-weighted magnetic resonance imaging predict a high gleason score of prostate cancer? *Korean J Urol* 2013;**54**(4):234–8. Page 20 of 51.
5. Thompson J, Lawrentschuk N, Frydenberg M, Thompson L, Stricker P. The role of magnetic resonance imaging in the diagnosis and management of prostate cancer. *BJU Int* 2013;**112**(2):6–20.
6. Vos EK, Litjens GJS, Kobus T, Hambrock T, Kaa CAH-VD, Barentsz JO, et al. Assessment of prostate cancer aggressiveness using dynamic contrast-enhanced magnetic resonance imaging at 3T. *Eur Urol* 2013;**64**(3):448–55.
7. Wibulpolprasert P, Phongkitkarun S, Chalermsanyakorn P. Clinical application of diffusion weighted- MRI in prostate cancer. *J Med Assoc Thail* 2013;**96**(8):967–75.
8. Kim CK, Takahashi S. Prostate cancer: predicting tumour aggressiveness using DWI-guided biopsy. *Nat Rev Urol* 2011;**8**(12):652–4.
9. Wallace TJ, Torre T, Grob M, Yu J, Avital I, Brucher BLDM, et al. Current approaches, challenges and future directions for monitoring treatment response in prostate cancer. *J Cancer* 2014;**5**(1):3–24.
10. Barentsz JO, Richenberg J, Clements R, Choyke P, Verma S, Villeirs G, et al. ESUR prostate MR guidelines. *Eur Radiol* 2012;**22**:746–57.
11. Costa DM, Bloch BN, Yao DF, Sanda MG, Ngo L, Genega EM, et al. Diagnosis of relevant prostate cancer using supplementary cores from magnetic resonance imaging-prompted areas following multiple failed biopsies. *Magn Reson Imag* 2013;**31**(6):947–52.
12. Durmus T, Reichelt U, Huppertz A, Hamm B, Beyersdorff D, Franiel T. MRI-guided biopsy of the prostate: correlation between the cancer detection rate and the number of previous negative TRUS biopsies. *Diagn Interventional Radiol* 2013;**19**(5):411–7.
13. Murphy G, Haider M, Ghai S, Sreeharsha B. The expanding role of MRI in prostate cancer. *Am J Roentgenol* 2013;**201**(6):1229–38.
14. Vargas HA, Akin O, Franiel T, Mazaheri Y, Zheng J, Moskowitz C, et al. Diffusion-weighted endorectal MR imaging at 3 T for prostate cancer: tumor detection and assessment of aggressiveness. *Radiology* 2011;**259**(3):775–84.
15. Verma S, Turkbey B, Muradyan N, Rajesh A, Cornud F, Haider MA, et al. Overview of dynamic contrast enhancement MRI prostate cancer diagnosis and management. *AJR* 2012;**198**:1277–88.
16. Villers A, Marliere F, Ouzzane A, Puech P, Lemaitre L. MRI in addition to or as a substitute for prostate biopsy: the clinicians point of view. *Diagn Interventional Imaging* 2012;**93**(4):262–7.
17. Bour L, Schull A, Delongchamps NB, Beuvon F, Muradyan N, Legmann P, et al. Multiparametric MRI features of granulomatous prostatitis and tubercular prostate abscess. *Diagn Interventional Imaging* 2013;**94**:84–90.
18. Puecha P, Sufana-Iancua A, Renarda B, Lemaitrea L. Prostate MRI: can we do without DCE sequences in 2013? *Diagn Interventional Imaging* 2013;**94**:1299–311.
19. Berman RM, Brown AM, Chang SD, et al. DCE MRI of prostate cancer. *Abdom Radiol (NY)* 2016;**41**(5):844–53.
20. Jeoung HK, Jung KR, Geon-Ho J, Jeong YS. Double inversion recovery MR imaging of the breast: efficacy in detection of breast cancer. *J Magn Reson Imaging* 2014;**39**:51–8.
21. Wattjes MP, Lutterbey GG, Gieseke J, Trä ber F, Klotz L, Schmidt S, et al. Double inversion recovery brain imaging at 3T: diagnostic value in the detection of multiple sclerosis lesions. *AJNR Am J Neuroradiol* 2007;**28**:54–9.
22. Madhuranthakam AJ, Sarkar SN, Busse RF, Bakshi R, Alsop DC. Optimized double inversion recovery for reduction of T1 weighting in fluid-attenuated inversion recovery. *Magn Reson Med* 2012;**67**:81–8.
23. Bojorquez JZ, Bricq S, Acquitter C, Brunotte F, Walker PM, Lalande A. What are normal relaxation times of tissues at 3 T? *Magn Reson Imaging* 2017;**35**:69–80.
24. Spektor M, Mathur M, Weinreb JC. Standards for MRI reporting-the evolution to PI-RADS v 2.0. *Transl Androl Urol* 2017;**6**(3):355–67.
25. Padhani AR, Weinreb J, Rosenkrantz AB, Villeirs G, Turkbey B, Barentsz J. Prostate imaging-reporting and data system steering committee: PI-RADS v2 status update and future directions. *Eur Urol* 2019 Mar;**75**(3):385–96.
26. Smith CP, Türkbey B. PI-RADS v2: current standing and future outlook. *Turk J Urol* 2018;**44**(3):189–94. https://doi.org/10.5152/tud.2018.12144.
27. Steiger P, Thoeny HC. Prostate MRI based on PI-RADS version 2: how we review and report. *Cancer Image* 2016;**16**:9.
28. Eman FD, Osama LN, Eman AG. Assessing the validity of Prostate Imaging Reporting and Data System version 2 (PI-RADS v2) scoring system in diagnosis of peripheral zone prostate cancer. *Eur J Radiol* 2017;**4**:19–26.
29. Hötker AM, Mazaheri Y, Aras O, Zheng J, Moskowitz CS, Gondo T, et al. Assessment of prostate cancer aggressiveness by use of the combination of quantitative DWI and dynamic contrast-enhanced MRI. *Am J Roentgenol* 2016;**206**(4):756–63.
30. Shayan SMA, Zahid AK, Rana SH, et al. *Assessment of apparent diffusion coefficient values as predictor of aggressiveness in peripheral zone prostate cancer: comparison with Gleason score*. ISRN Radiology; 2014, 263417.
31. Wua X, Reinikainena P, Vanhanena A, Kapanena M, Vierikkob T, Ryyminb P, et al. Correlation between apparent diffusion coefficient value on diffusion-weighted MR imaging and Gleason score in prostate cancer. *Diagn Interventional Imaging* 2017;**98**:63–71.
32. Afaq A, Koh DM, Padhani A, Van ASN, Sohaib SA. Clinical utility of diffusion-weighted magnetic resonance imaging in prostate cancer. *BJU Int* 2011;**108**(11):1716–22.
33. Borren A, Groenendaal G, Moman MR, Boeken KAE, Van DPJ, Van VM, et al. Accurate prostate tumour detection with multiparametric magnetic resonance imaging: dependence on histological properties. *Acta Oncol* 2014;**53**(1):88–95.
34. Charles-Edwards EM, deSouza NM. Diffusion-weighted magnetic resonance imaging and its application to cancer. *Cancer Image* 2006;**6**:135–43.
35. Ibrahiem EI, Mohsen T, Nabeeh AM, Osman Y, Hekal IA, Abou El-Ghar M. DWI-MRI: single, informative, and non-invasive technique for prostate cancer diagnosis. *Sci World J* 2012;**2012**:1537.
36. Kitajima K, Takahashi S, Ueno Y, Yoshikawa T, Ohno Y, Obara M, et al. Clinical utility of apparent diffusion coefficient values obtained using high b-value when diagnosing prostate cancer using 3 tesla MRI: comparison between ultra-high b-value (2000 s/mm2) and standard high b-value (1000 s/mm2). *J Magn Reson Imaging* 2012;**36**(1):198–205.
37. Maas MC, Futterer JJ, Scheenen TWJ. Quantitative evaluation of computed high b value diffusion weighted magnetic resonance imaging of the prostate. *Investig Radiol* 2013;**48**(11):779–86.
38. Murphy G, Haider M, Ghai S, Sreeharsha B. The expanding role of MRI in prostate cancer. *Am J Roentgenol* 2013;**201**(6):1229–38.
39. Olivera NJA, Parente DB. Multiparametric magnetic resonance imaging of the prostate. *Magn Reson Imag Clin N Am* 2013;**21**(2):409–26.
40. Padhani AR, Liu G, Mu-Koh D, Chenevert TL, Harriet C, Thoeny HC, et al. Diffusion-Weighted Magnetic resonance imaging as a cancer biomarker: consensus and Recommendations. *Neoplasia* 2009;**11**(2):102–25.
41. Peng Y, Jiang Y, Yang C, Brown JB, Antic T, Sethi I, et al. Quantitative analysis of multiparametric prostate MR images: differentiation between prostate cancer and normal tissue and correlation with Gleason score- A computer-aided diagnosis development study. *Radiology* 2013;**267**(3):787–96.
42. Quentin M, Schimmoller L, Arsov C, Rabenalt R, Antoch G, Albers P, et al. Increased signal intensity of prostate lesion on high b-value diffusion weighted images as a predictive sign of malignancy. *Eur Radiol* 2014;**24**(1):209–13.
43. Rais-Bahrami S, Siddiqui MM, Turbey B, Stamatakis L, Logan J, Hoang AN, et al. Utility of multiparametric magnetic resonance imaging suspicion levels for detecting prostate cancer. *J Urol* 2013;**190**(5):1721–7.
44. Somford DM, Hambrock T, Hulsbergen-Van de Kaa CA, Futterer JJ, van Oort IM, van Basten JP, et al. Initial experience with identifying high-grade prostate cancer using diffusion-weighted MR imaging (DWI) in patients with a Gleason score <3+3=6 upon schematic TRUS-guided biopsy: a radical prostatectomy correlated series. *Investig Radiol* 2012;**47**(3):153–8.
45. Somford DM, Hoeks CM, Hulsbergen-Van De Kaa CA, Hambrock T, Futterer JJ, Witjes JA, et al. Evaluation of diffusion-weighted MR imaging at inclusion in an active surveillance protocol for low-risk prostate cancer. *Investig Radiol* 2013;**48**(3):152–7.